# Density functional theory study of graphite oxide for different oxidation levels

R. J. W. E. Lahaye,* H. K. Jeong,† C. Y. Park, and Y. H. Lee‡
*Department of Physics, Department of Energy Science, Center for Nanotubes and Nanostructured Composites, Sungkyunkwan University, Suwon 440-746, Korea*

(Received 22 October 2008; revised manuscript received 11 February 2009; published 27 March 2009)

Graphite oxide constitutes a hexagonal carbon network with oxygen atoms in carbon-oxide ether ring formations and hydroxyl molecules. We have studied graphite oxide with a first-principles density functional theory calculation for different oxidation levels. The oxygen atoms form 1,2-ether groups (epoxides) on the carbon grid, with on the adjacent carbon atoms, but at the opposite side of the carbon plane, the hydroxyl molecules. Graphite oxide cannot have 1,3-ether oxygens because of the higher formation energy. The transverse wrinkling of the carbon grid is about 0.5 Å, mostly due to the deformation around the hydroxyl bonds, yet the in-plane lattice axes retain the hexagonal features of graphene. A stable graphite oxide structure requires hydroxyl molecules to relax the tension on the carbon grid from the 1,2-ether oxygens. At a low degree of oxidation, graphite oxide is a semiconductor, but when the oxidation is saturated, it turns into an insulator.

DOI: 10.1103/PhysRevB.79.125435 PACS number(s): 68.47.Gh, 61.50.Ah

## I. INTRODUCTION

Renewed interest in graphite oxide (GO) has been sparked by recent discoveries of surprising electronic properties of graphene,[1–4] a single atomic layer of graphitic carbon. As a result a quest has started for techniques to efficiently extract and manipulate single graphene layers. GO is a promising candidate as a precursor to making graphene platelets. Unlike graphite, GO easily exfoliates and disperses in an aqueous solution, and a subsequent chemical reduction opens opportunities to synthesize individual platelets of a graphenelike material.[5–7] A thorough knowledge of the GO base material, in particular its structural and electronic properties, is therefore a prerequisite.

Graphite oxide has been studied ever since its first synthesis by Brodie in the mid 1800s.[8] Over the years various structural models have been proposed,[9–14] which by now has merged into a general understanding that oxygen atoms and hydroxyl molecules are the key species on a laminar carbon network, which adopts a wrinkled hexagonal structure with typically 6–7 Å distance between the layers.[15–17] The ratio of carbon and oxygen atoms is the yardstick of the oxidation efficiency. In progressively oxidized GO this ratio approaches the value of 2,[17] whereas chemically reduced GO platelets are reported to have C/O ratios up to 10.[5,6] Fully oxidized graphite has thus a coverage of the carbon network of approximately 50% and its ideal chemical composition is $C_8O_2(OH)_2$ or $C_6O(OH)_2$.[15,18,19] Intercalated water molecules, however ubiquitous in this hydrophilic material, have marginal effects on the structure of the individual layers, but moderate the interlayer distance.[17,18,20]

Much work has been done on investigating experimentally the precise arrangement of the oxygen atoms and hydroxyl molecules on the carbon network of GO. The hydroxyl molecules undoubtedly are located on top of individual carbon atoms in a more or less upright position with respect to the carbon plane. However, the position of the single oxygen atoms is still ambiguous. They are either in a 1,2-ether or a 1,3-ether location, where the numbering scheme refers to a three-member C-O-C ring (epoxide) and a four-member carbon-oxide ring, respectively. Experiments cannot distinguish between the two oxygen species and assignments have been made either way without reaching a consensus.[15–17,21–23]

Experimental work on GO outnumbers the attempts by theoretical modeling, which mostly have studied oxidized graphite[24–27] instead of more realistic models of GO as proposed by experiments. Neglecting the presence of hydroxyl molecules in the models makes the theoretical results of limited relevance to a better understanding of GO. A thorough theoretical study into stable structures of GO must include both oxygen atoms and hydroxyl molecules in the models.[6,19] A systematical study and comparison of different structure configurations of GO is still missing and is relevant to the understanding of experimental data. In particular a theoretical study has not yet been conducted into the 1,2-ether and 1,3-ether arrangements of the carbon-oxygen rings in GO.

In present work we use density functional theory (DFT) to study the structure of GO in order to find a theoretical footing for the configuration and arrangement of hydroxyls and oxygens on the GO layers in the light of the 1,2-ether versus 1,3-ether oxygen ambiguity. A supercell of eight carbon atoms forms a hexagonal graphitic carbon frame. Ether and hydroxyl groups are then placed at approximate locations, followed by an energy relaxation to obtain the equilibrium positions. Two types of GO are studied: a low degree of oxidation, with one ether and one hydroxyl in the supercell, and saturated oxidation, with two ethers and two hydroxyls in the supercell.

## II. COMPUTATIONAL METHOD

For the molecular modeling, we have used the *ab initio* total-energy calculation and molecular-dynamics program VASP (Ref. 28) with the projector-augmented wave (PAW) method[29–32] for pseudopotentials of the core electrons and the plane-wave basis sets of the valence electrons. The package implements the density functional theory with the generalized gradient approximation for the exchange and correlation in the Perdew-Burke-Ernzerhof formalism.[33–35] The

 

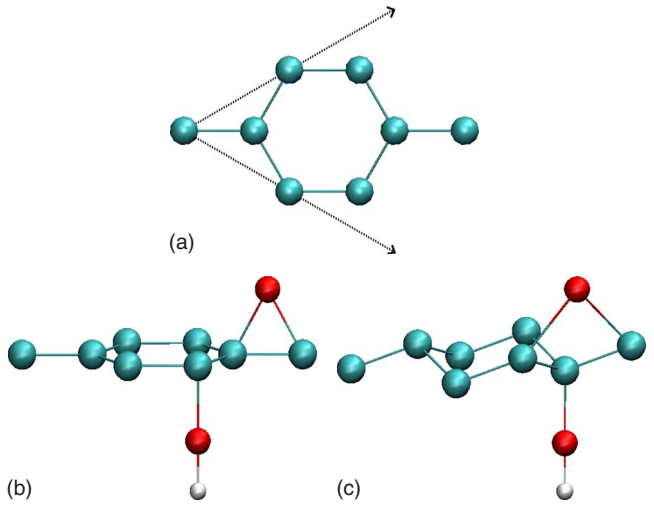


FIG. 1. (Color online) The graphene supercell of eight carbon atoms in panel (a) forms the basic structure for setting up the GO unit cell. The in-plane lattice vectors, shown as arrows, are 5 Å long and make an angle of 60°. Panels (b) and (c) show two examples of GO with one ether oxygen and one hydroxyl (1,2-ether and 1,3-ether configuration, respectively) prior to the energy relaxation of the atom positions.

Brillouin zone is sampled with 41 irreducible $k$ points, chosen from the two-dimensional $9\times9\times1$ Monkhorst-Pack mesh.[36] A plane-wave cutoff energy of 400 eV for all atoms guarantees a total-energy accuracy in the order of 10 meV. The positions of the nuclei in the initial structures were first relaxed by the conjugate-gradient algorithm, until the Hellman-Feynman forces on each nucleus were less than 0.01 eV/Å.[37–39] Using a plane-wave cutoff energy of 520 eV during the relaxation, we can also optimize the shape of the unit cell at a constant volume. After the relaxation a spin-polarized total energy of the electronic structure was calculated using a self-consistent field method that terminated when change in total energy between two subsequent steps was less than $10^{-5}$ eV. Binding energy between two species follows from the general procedure of total-energy difference between the two constituents and the structure as a whole, where each total-energy calculation is preceded by a relaxation.

The procedure to construct the unit cell of GO is shown in Fig. 1. The unit cell has a frame of eight carbon atoms arranged in a hexagonal configuration, i.e., a graphene supercell, with 10 Å between the layers to depreciate interlayer interactions. Ether oxygen atoms are positioned between two carbon atoms at an approximate height of 1.3 Å, and hydroxyls are on top of a carbon atom with a C-O distance of 1.5 Å and an O-H separation of 1 Å. Initially the nascent carbon structure is flat when simulating structures with 1,2-ether oxygens [Fig. 1(b)], but to tailor 1,3-ether oxygen configurations the carbon atoms are initially in a wrinkled zigzag-chair formation [Fig. 1(c)]. In case of a low degree of oxidation, there is one oxygen atom and one hydroxyl molecule per unit cell. Saturated oxidation requires two oxygens and two hydroxyls in the unit cell. The final equilibrium positions of all atoms in the structure follow from a subsequent structure relaxation, while maintaining an interlayer distance of 10 Å.

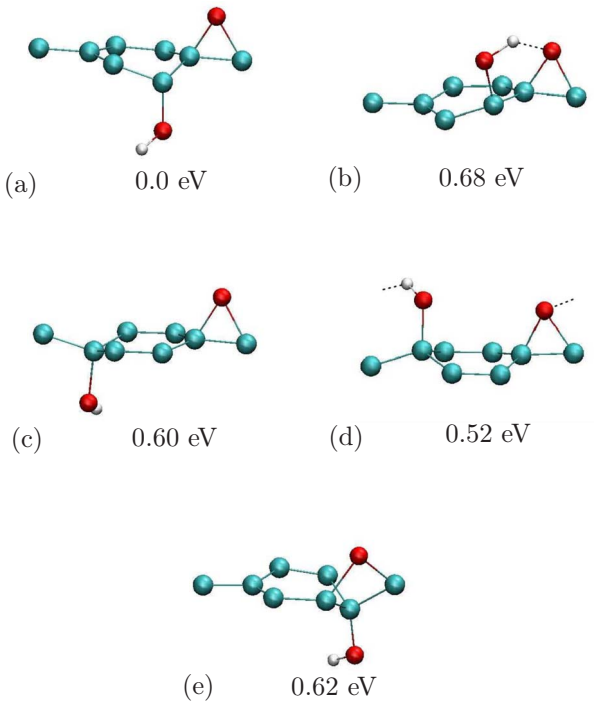


FIG. 2. (Color online) The five stable configurations of GO with one ether oxygen and one hydroxyl in the unit cell of eight carbon atoms. Panels (a)–(d) have 1,2-ether oxygens, and (e) has a 1,3-ether. The dotted lines in panels (b) and (d) indicate intralayer hydrogen bonds between the ether oxygen and the hydrogen atom of the hydroxyl. The energy labels in the figure are the total energies relative to the most stable configuration of panel (a).

Periodic boundary conditions replicate the unit cell into an infinite layered hexagonal network. This also imposes a periodic pattern of the oxidation. In reality, however, the oxidation process distributes the oxygens and hydroxyls randomly across the carbon grid.[12,40] We have verified in our calculations that a larger GO unit cell (16 or 32 carbon atoms) does not produce a different geometric structure. Choosing a unit cell of eight carbon atoms allows us to systematically investigate and compare a variety of different structure configurations.

## III. RESULTS FOR LOW OXIDIZED GO

The elementary unit cell of the GO layer in our model contains eight carbon atoms in a hexagonal arrangement. This basic structure of carbon atoms is then decorated with a single oxygen atom and a single hydroxyl molecule. The C/O ratio of 4 represents a low oxidation level of GO.

In case of a 1,2-ether position of the oxygen atom, the number of possible locations for the oxygen and hydroxyl narrows down to four due to the symmetry in the unit cell. Figures 2(a)–2(d) show the relaxation results (atom positions of minimum total energy). A similar number of configurations exists with the oxygen atom in a 1,3-ether position, but all are unstable except for the one shown in Fig. 2(e). The energy labels in the figure panels are the structure's total energy relative to the one with the lowest total energy in Fig. 2(a).

Most GO configurations with a 1,3-ether oxygen are unstable and, upon relaxation, spontaneously evolve into a 1,2-ether oxygen. Although the carbon atoms are wrinkled in a zigzag pattern before relaxation, to help survive the 1,3-ether configuration, the carbon atoms still tend to restore a flat structure during the relaxation. Then on such a flat carbon plane the oxygen easily establishes a bond with the second carbon atom in the ether ring, because that distance becomes shorter than the intended C-O bond with the 1,3-carbon atoms. The single exception to this transformation occurs when the hydroxyl molecule "occupies" the second carbon atom in the 1,3-ether ring, as shown in Fig. 2(e). The hydroxyl molecule perseveres in the deformation of the carbon plane, which locally adopts the $sp^3$ coordination, and this prevents the 1,3-ether oxygen to create a bond with the second carbon atom in the ether ring. Consequently, this construct requires that the corresponding oxygen and hydroxyl reside at opposite sides of the carbon plane in a close-packed formation. Although this is the only stable structure with a 1,3-ether oxygen, its total energy is higher than most other structures with 1,2-ether oxygens.

The structure in Fig. 2(a) has the lowest total energy and thus is the most probable configuration for GO. It has the hydroxyl immediately adjacent to the 1,2-ether oxygen, but at the opposite side of the carbon sheet (*trans*configuration). This confirms and refines an important experimental result that the two species must be very close to one another.[16,23,40] The structure in Fig. 2(b) differs from the previous one in that the hydroxyl is on the same side as the ether oxygen (*cis*configuration). Such a configuration, however, creates tension on the carbon-carbon bonds, because all three carbon atoms attached to an oxygen elevate out of the carbon plane in the same direction. This frustrates the desired $sp^3$ hybridization of the carbon atom attached to the hydroxyl and the tension increases the total energy by 0.68 eV. For the structures in Figs. 2(c) and 2(d), the hydroxyl is located farther away from the ether oxygen. This also leads to more tension in the carbon grid and it increases the total energy by 0.60 and 0.52 eV, respectively.

An oxygen atom on flat graphene (without hydroxyl) forms a 1,2-ether bond with the carbon atoms. The binding energy of the oxygen is then 2.1 eV, previously reported as 1.9 and 2.4 eV.[24,27] A hydroxyl alone on graphene, on the other hand, turns out to have a binding energy of 0.7 eV. The coadsorption of both the oxygen atom and hydroxyl molecule leads to a stronger concerted binding energy than conjectured from the separate bonds, which is in agreement with simulation work by Boukhvalov and Katsnelson.[19] For the structure with the lowest total energy in Fig. 2(a), the joint binding energy of the oxygen and hydroxyl is 3.6 eV (an 0.8 eV gain with respect to the individual species), whereas this binding energy is merely about 3.1 eV (0.3 eV gain) for the other structures in Fig. 2. In the latter cases the conjoint binding energy is less due to the extra stress on the carbon network. From this we conclude that for the structure as a whole the tension on the carbon grid is the most relevant factor in lowering the total energy and obtaining a stable configuration of GO.

Intralayer hydrogen bonds are feasible only when the hydroxyl and 1,2-ether oxygen are in a cisconfiguration, as shown in Figs. 2(b) and 2(d). Note that hydrogen bonds between different layers are negligible in our model because the large interlayer distance separates oxygens and hydroxyls by at least 6 Å. The distance between the hydrogen atom and the ether oxygen in Figs. 2(b) and 2(d) is 1.8 Å. This hydrogen bond is too weak to be relevant to the stability of the structure because both configurations with hydrogen bonds have a higher total energy than the configuration without hydrogen bonds in Fig. 2(a). Hence, the hydroxyl molecules primarily minimize their total energy by adjusting the bond angle to approximately 110° with respect to the C-O bond, conform to the geometry of an oxygen atom with two single bonds.

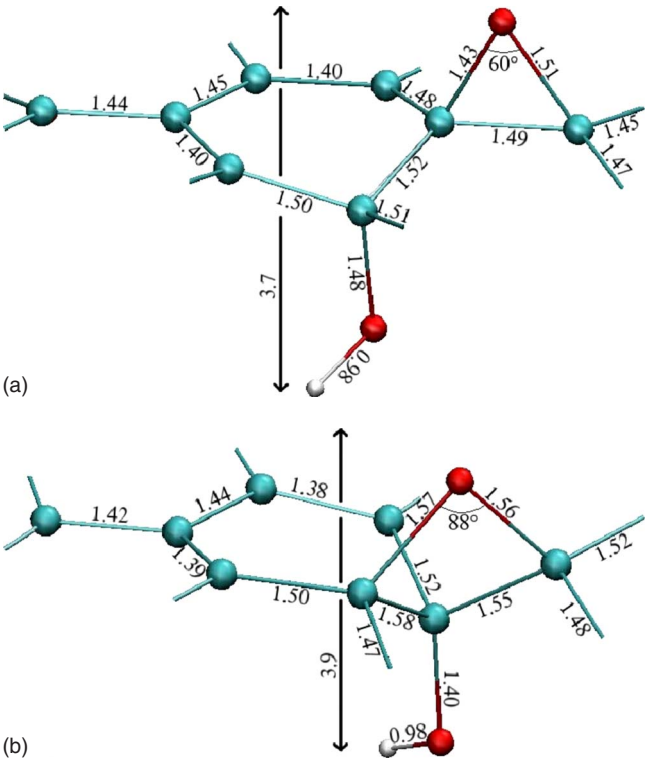


FIG. 3. (Color online) Detailed geometric arrangement of the two GO structures with a 1,2- and 1,3-ether oxygen from Figs. 2(a) and 2(e), respectively. The interatomic distances are in angström.

We have evaluated the geometric perturbation of the carbon atoms in the GO structures by a least square fit to a flat plane. The maximum distance between the outermost carbon atoms above and below the best-fit plane is a measure of how much the GO structure is wrinkled in the transverse direction with respect to a flat carbon grid. The 1,3-ether configuration of Fig. 2(e) is wrinkled most by 0.9 Å, whereas for the 1,2-ether configurations [Figs. 2(a)–2(d)] this is 0.4 Å. Additional simulations reveal that the wrinkling of the carbon grid with just a single 1,2-ether oxygen is 0.12 Å and with only a hydroxyl on the carbon grid we found 0.21 Å. Therefore the hydroxyl molecule causes most of the wrinkling of the carbon frame, but the coadsorption of the oxygen and hydroxyl causes more wrinkling than inferred from their individual contributions.

Figure 3 illustrates in more detail the geometric properties of the structures with the 1,3-ether oxygen and the 1,2-ether

TABLE I. Summary of the results for the 1,2- and 1,3-ether oxygen in low oxidized GO structures of Figs. 2(a) and 2(e): the total binding energy of the structure ($E_{tot}$), the binding energy of the ether oxygen and hydroxyl with the carbon frame ($E_{O/OH}$), the wrinkling of the carbon grid ($W$), the C-O-C bond angle ($\angle$), the average C-C bond lengths of the immediate adjacent carbon atoms at the ether oxygen and the hydroxyl ($\langle$C-C$\rangle$), and the electronic band gap at the Fermi energy between equal spins (left value) and opposite spins (right value). Energies and distances are in electronvolts and angström, respectively. See text for further details.

| | | | | C-O-C | | C-OH | band gap | |
|---|---|---|---|---|---|---|---|---|
| GO | $E_{tot}$ | $E_{O/OH}$ | $W$ | $\angle$ | $\langle$C-C$\rangle$ | $\langle$C-C$\rangle$ | at $E_f$ | |
| 1,2-ether | 0.0 | 3.6 | 0.4 | 60° | 1.48 | 1.51 | 1.4 | 0.4 |
| 1,3-ether | 0.62 | 3.1 | 0.9 | 88° | 1.52 | 1.55 | 0.7 | 0.0 |

oxygen [the latter is the lowest energy configuration from Fig. 2(a)]. The two configurations have in common that the oxygen and hydroxyl pair up on neighboring carbon atoms at opposite sides of the carbon plane. Also, the carbon atoms far from the oxygen-hydroxyl pair resemble the flat geometry of graphene with C-C bond lengths between 1.38 and 1.45 Å, although the short bond lengths of around 1.38 Å rather indicate double bonds (C=C) of a conjugated carbon structure. Differences between the two structures occur in the C-C bond lengths near the oxygen and the hydroxyl. In case of the 1,3-ether structure these C-C distances are closer to the 1.54 Å distance of diamond, confirming that this structure locally has a much stronger $sp^3$ hybridization (see also Table I). This causes longer C-O bond lengths in the 1,3-ether ring, but shortens somewhat the C-O distance with the hydroxyl, when compared to the distances in the 1,2-ether structure.

Another notable difference between the two structures in Fig. 3 is the C-O-C angle in the ether ring, also listed in Table I. An angle of 88° in the 1,3-ether oxygen is supposed to have less strain than the 60° in the 1,2-ether oxygen. The optimum C-O-C angle is about 110° and from molecular chemistry one learns that 1,3-ether oxygens are more stable and less reactive than equivalent 1,2-ethers. In GO, however, the 1,3-ether configuration is only feasible when the second carbon atom in the four-member ring can move farther away from the oxygen. This is difficult in a rigid carbon frame, but the hydroxyl molecule can do this by inducing an $sp^3$ hybridization. It steers the carbon atom away from the ether oxygen and the 1,3-ether configuration remains stable at the cost of extra strain in the carbon network. Without the assistance of such a hydroxyl molecule, the geometry of the carbon atoms only permits 1,2-ether oxygens.[6,24]

The strain in the 1,2-ether ring exercises a cleaving force on the two carbon atoms. If the ether oxygen lines up with the ones on neighboring carbon hexagons, they can create a fault line in the carbon plane.[27] Such a process coined as "unzipping of graphite" causes cracks in the graphite structure, which eventually leads to small GO platelets. This must occur in regions where the ether oxygens dominate over the hydroxyl molecules. It is then a reasonable assumption that the hydroxyl molecules are a stabilizing factor, which stops a continuation of the cracking process and prevents a total breakdown of the carbon network.

The distance between the outermost oxygen and hydrogen atoms in Fig. 3 is an indication of the thickness of the GO layer. This layer thickness is 3.7 and 3.9 Å for the 1,2-ether and 1,3-ether oxygen structures, respectively. The experimentally measured interlayer distance is 6 Å (or somewhat less when the amount of intercalated water is small),[17] and thus the interstitial void in between the GO layers is then roughly 2–3 Å. This is barely enough space to accommodate water molecules that connect the layers via hydrogen bonds, of which the bond distance is also about 2 Å. The few water molecules that subsist in dry GO cannot be mobile and must be firmly anchored in the structure. We surmise that this explains the experimentally observed immobility of certain water molecules in GO independent of temperature.[20] Possibly such rigid water molecules play a key role in the stability of the laminar formation of the GO structure.

Before obtaining the total energy of a structure, the positions of the nuclei are relaxed into a configuration where the forces are small (less than 0.01 eV/Å). Besides maneuvering all atoms into their equilibrium positions, the total-energy minimization also adjusts the shape of the GO unit cell to the new positions of the atoms. In fact, this only affects the area and angle spanned by the in-plane lattice vectors [as shown in Fig. 1(a)] since the enforced interlayer distance of 10 Å is too large to influence the total energy through changes along the $c$ axis. All structures with the 1,2-ethers maintain the 60° angle between the in-plane lattice vectors, but undergo a 2% increase in the spanned area, with respect to an equilibrium graphite structure. This increase can be attributed to the extended carbon-carbon bonds around the hydroxyl and the ether ring. In case of the 1,3-ether, the stronger wrinkling leads to a 2% decrease in the area with an angle of 61°. All these changes in the unit cell are fairly small. Also in experiments, the carbon atoms in GO show a nearly perfect hexagonal structure.[12,40] Thus by and large the hexagonal dimensions of the in-plane carbon frame in GO are still close to the one of graphene despite the wrinkled geometry.

Oxygen atoms have a larger electronegativity than carbon atoms. GO becomes a $p$-doped material where the charge flow creates negative oxygen atoms and a positively charged carbon grid. Unfortunately we cannot quantify the net charges theoretically because *ab initio* calculations with plane-wave basis sets have the drawback that charge transfer is not uniquely defined; the local charge on an atom is the integration of the charge density in an arbitrary spherical volume around its nucleus and thus absolute values of charge

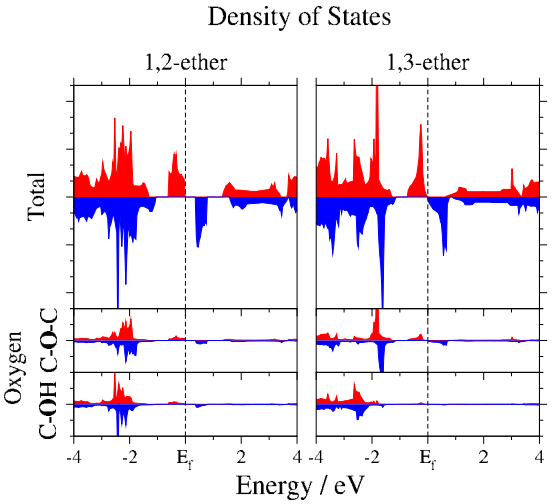


FIG. 4. (Color online) Density of states, with the majority and minority spins separated, for the two structures in Fig. 3. The upper panels represent the total density of states for all atoms in the unit cell, whereas the two lower panels are the partial density of states for the oxygen atoms separated into the ether oxygens and the oxygen in the hydroxyl molecules. The abscissa is cropped at 4 eV from the Fermi energy.

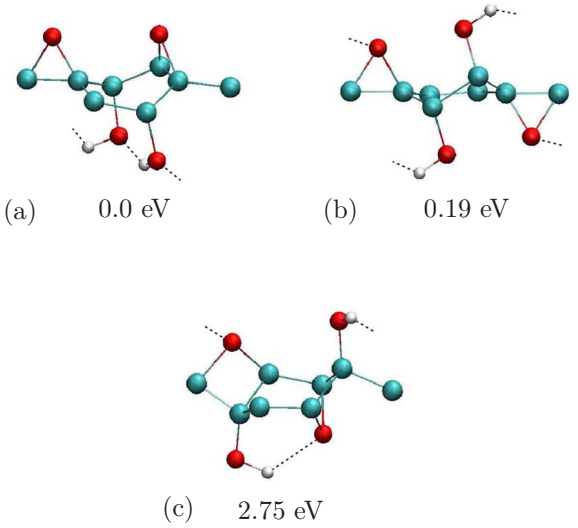


FIG. 5. (Color online) Three examples of the graphite oxide unit cell with two ether oxygens and two hydroxyls. Panels (a) and (b) are the configurations with the lowest total energy and have the oxygen atoms in the 1,2-ether locations; panel (c) has the oxygens in the 1,3-ether location. The dotted lines indicate intralayer hydrogen bonds between the ether oxygen and the hydrogen atom of the hydroxyl. The energy labels refer to the total energy relative to the structure in panel (a).

transfer have no meaning. However, comparing charge differences for a fixed volume radius gives valid qualitative trends. A radius of 0.863 Å for the carbon atom is a practical compromise between maximizing the covered space and minimizing the overlap of the spheres. We integrate the charge distributions on all carbon atoms for both graphite and GO, and the difference renders the relative charge flow from the carbon grid to the oxygen atoms. The corresponding charge distribution is calculated for the structures of Fig. 2 and it follows the trend of the total energy, in the sense that the least charge transfer from the carbon to the oxygen atoms corresponds to the lowest total energy. The structure with the lowest total energy [Fig. 2(a)] has the transconfiguration and the antipodal positions of the two oxygens may cause the minimal charge transfer.

The electronic energy distribution of GO is depicted in Fig. 4 as the density of states and the band gap at the Fermi energy is given in Table I. The exchange interaction causes an energy shift of the two electron-spin states, resulting in an unpaired electron per unit cell for both the 1,2-ether and 1,3-ether configurations. If we neglect the possibility of spin flipping, then the energy gap of the majority spin at the Fermi level is 1.4 and 0.7 eV for the 1,2-ether and 1,3-ether configurations, respectively, which is the characteristic band gap of a semiconductor. If, on the other hand, the ambient conditions allow spin flips, then the band gap shrinks to 0.4 and 0 eV for the two respective structures. The states of the unpaired electron are near the Fermi energy. Because partial states of the oxygen atoms have very little contribution in that region, the unpaired electron predominantly resides on the carbon atoms, in particular the ones farthest away from the oxygen or hydroxyl adsorption sites.

The shift of the majority and minority spins is an interesting feature that allows us to predict magnetic properties for this type of GO, which scale with one Bohr magneton per 21 $Å^2$, i.e., a single unpaired electron per unit cell of eight carbon atoms. We have not investigated further on whether this type of GO is ferro- or paramagnetic.

## IV. RESULTS FOR SATURATED OXIDIZED GO

The chemical composition of fully oxidized GO is close to $C_8O_2(OH)_2$.[15,18,19] This requires an augmentation of the preceding model with an additional ether oxygen and another hydroxyl molecule. The number of permutations for the different structure configurations grows notably with the additional two species in the unit cell. Here we will discuss a few structures of interest, collated in Fig. 5, namely, two configurations with the lowest total energy, which both appear to have 1,2-ether oxygens, and a structure with 1,3-ether oxygens that has a much higher total energy. The two structures with the 1,2-ether configurations demonstrate again that the ether oxygens and the hydroxyls prefer to obey the transconfiguration, i.e., the hydroxyls are attached to a carbon atom directly adjacent to the ether oxygen, but at opposite side of the carbon plane. The main difference between the two structures is that the lowest total energy has all ether oxygens at one side and all hydroxyls at the other side of the carbon plane, whereas a slight increase in the total energy by 0.19 eV occurs when the species are located at alternate sides of the carbon plane.

Most structures with 1,3-ether oxygens are unstable and transform to 1,2-ether oxygens during the relaxation. The structure in Fig. 5(c) is the only exception due to the fact that the hydroxyl molecules, attached to the carbon atom in the 1,3-ether ring, prevent the transformation to a 1,2-ether configuration. The total energy of this configuration is 2.75 eV

TABLE II. Summary of the results for the 1,2- and 1,3-ether oxygen in saturated oxidized GO structures of Figs. 5(a) and 5(c): the total binding energy of the structure ($E_{tot}$), the wrinkling of the carbon grid ($W$), the C-O-C bond angle ($\angle$), the average C-C bond lengths of the immediate adjacent carbon atoms at the ether oxygen and the hydroxyl ($\langle$C-C$\rangle$), and the electronic band gap at the Fermi energy. Energies and distances are in electronvolts and angström, respectively. See text for further details.

| | | | C-O-C | | C-OH | band gap |
|---|---|---|---|---|---|---|
| GO | $E_{tot}$ | $W$ | $\angle$ | $\langle$C-C$\rangle$ | $\langle$C-C$\rangle$ | at $E_f$ |
| 1,2-ether | 0.0 | 0.6 | 62° | 1.50 | 1.53 | 3.2 |
| 1,3-ether | 2 75 | 1.0 | 86° | 1.53 | 1.54 | 1.7 |

higher than the lowest total energy with the 1,2-ether oxygens. This attests again that 1,3-ether oxygens are energetically very improbable in GO.

Another interesting instability happens when two hydroxyls form a vicinal diol on the same side of the carbon plane. This weakens the bonds between the oxygen and the carbon atoms such that during the structure relaxation both hydroxyl molecules detach from the carbon grid. Hence, two hydroxyl molecules at the same side of the carbon plane must be in parapositions [separated by one or more carbon atoms, like in Fig. 5(a)]; this restriction does not apply to hydroxyls positioned at alternate sides of the carbon plane as in Fig. 5(b). More than two hydroxyl molecules per carbon hexagon cause too much tension in the carbon grid and result in a spontaneous detachment of at least one hydroxyl from the carbon plane. This seems to disagree with previously proposed theoretical models,[6,19] but is in line with experimental analysis.[18]

Interactions between dangling hydrogens and oxygen atoms is inevitable in saturated oxidized GO. Figure 5 shows the hydrogen bonds between an ether oxygen and a hydroxyl, or between two hydroxyls. In all cases, the distance between the hydrogen and the oxygen atoms is about 1.95 Å. It is even larger than the 1.8 Å distance for hydrogen bonds in low oxidized GO. We therefore conclude that intralayer hydrogen bonds also in saturated oxidized GO do not play a significant role in the stability of the structure.

The carbon frames in Fig. 5 have a wrinkling of 0.6 and 1.0 Å for the 1,2-ether and 1,3-ether oxygen configurations, respectively, whereas this was 0.4 and 0.9 Å for the structures with only one oxygen and one hydroxyl (Fig. 2). The extra oxygen and hydroxyl cause a small additional wrinkling of the carbon plane. Although both 1,2-ether structures in Fig. 5 have a similar amount of wrinkling, the nature of the wrinkling is rather different, owing to the different locations of the hydroxyl molecules. In Fig. 5(a) the wrinkling of the carbon grid is more the type of a smooth chair-shape across the whole unit cell, whereas in Fig. 5(b) the wrinkling is localized on two carbon atoms only, with the rest of the unit cell fairly flat.

The thickness of the layer, defined as the distance between the outermost atoms, depends on which site of the carbon plane the oxygen atoms and hydroxyl molecules are located. The distance is about 3.6 Å for oxygens and hydroxyls at opposite sides of the carbon plane [Fig. 5(a)], and becomes 4.5 Å for the alternating orientations [Fig. 5(b)]. For the structure with 1,3-ether oxygens [Fig. 5(c)] it is even 4.9 Å. The layer thickness is largest, when the hydroxyls reside at both sides of the carbon plane, because the dangling hydrogens in the hydroxyl molecules protrude more than the ether oxygens.

The C-O-C angle of the ether rings in Fig. 5 is listed in Table II. They exhibit the same characteristics as their counterparts for low oxidized GO in Fig. 3. Both 1,2-ether configurations in Figs. 5(a) and 5(b) have C-O-C angles of 62°, whereas these angles are 86° for the 1,3-ether configuration in Fig. 5(c). The configuration of GO with the lowest total energy is the one with the highest tension in the C-O-C ether ring.

The bond distances in the carbon frame are shown in Fig. 6 for the particular case of the structure in Fig. 5(a), although the other structures in Fig. 5 exhibit similar properties. The ether oxygens and hydroxyls in the unit cell have a significant effect on the distances between the carbon atoms. Most of the carbon-carbon distances are extended, compared to graphite, because most carbons become $sp^3$ hybrids due to a bond with an oxygen atom. Interatomic distances for the ether oxygen atoms or the hydroxyl molecules are not indicated, but they are similar to those depicted in Fig. 3. All distances between carbon atoms are about 1.5 Å, except one that is 1.36 Å. The longest bonds represent a nearly complete $sp^3$ hybridization and occur around the carbons with

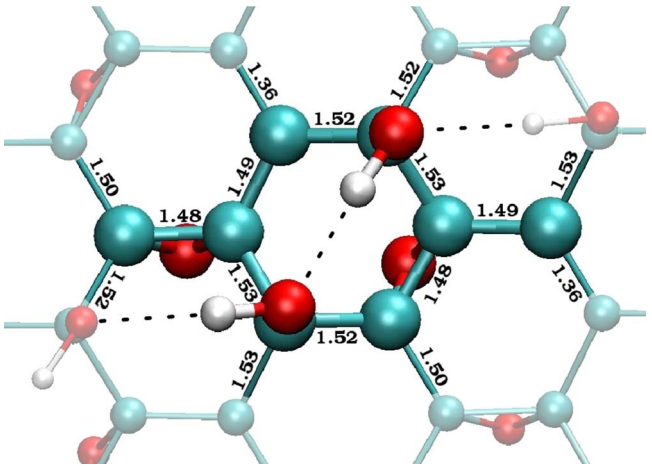


FIG. 6. (Color online) Distances between the carbon atoms for the GO structure of Fig. 5(a). The atoms in the unit cell are accentuated by size and brightness. The dotted lines represent hydrogen bonds between oxygens and hydrogens of adjacent hydroxyls. Distances are in angström.

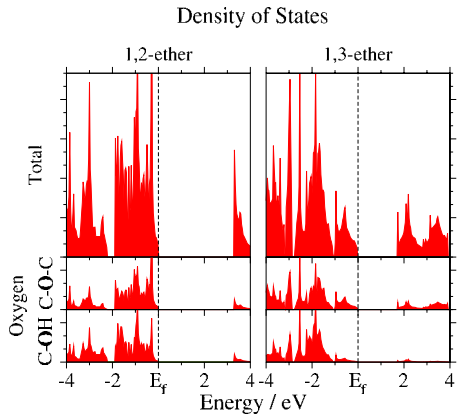


FIG. 7. (Color online) The electronic density of states around the Fermi energy for the 1,2-ether and 1,3-ether structures of Figs. 5(a) and 5(c), respectively. The total density of states is the sum over all atoms in the unit cell, and the partial density of states is for the oxygen atoms in the ether ring and in the hydroxyl molecule. The abscissa is cropped at 4 eV from the Fermi energy.

the hydroxyls. The short bond of 1.36 Å indicates a double bond between two carbon atoms and implies a conjugated carbon network. Each structure in Fig. 5 has one such double bond per unit cell.

As for the two cases with the lowest total energy [Figs. 5(a) and 5(b)], the in-plane geometry of the carbon skeleton in the unit cell is still very close to graphene. The angle between the unit vectors remains 60° and the area spanned by these vectors is 4% larger compared to graphene. The intensive wrinkling in the structure with the 1,3-ether oxygens has a different impact on the shape of the unit cell. Both angle and spanned area by the in-plane unit vectors contract to 58° and 4% smaller area. Overall, these deviations from the graphene unit cell are small and thus the in-plane dimensions of the unit cell in GO closely resemble those of graphene.

The two oxygen atoms and two hydroxyl molecules in the unit cell make all the electron spins pair up and therefore unpaired electrons are not present in the structures of Fig. 5. Consequently, magnetic properties due to spin polarization cannot exist. Besides the three structures shown in Fig. 5, there are many other structures with a different arrangement of the oxygens and hydroxyls, all with a much higher total energy. A few of those actually do have unpaired electrons, but their high total energies should prohibit the formation of such structures. In contrast, when only one ether oxygen and one hydroxyl exist in the unit cell (Fig. 2), the structures with the lowest total energy exhibit a spin polarization. Hence, the vanishing of magnetic properties is an important difference between partially and fully oxidized GO.

The spin-unresolved densities of states in Fig. 7 exhibit a large band gap of 3.2 eV for the 1,2-ether configuration and a much smaller band gap of 1.7 eV for the 1,3-ether configuration. It is known from experiments that the conductivity of graphite decreases with increasing oxidation.[6,7,41] Fully oxidized GO becomes an insulator, in contrast to low oxidized GO that is a semiconductor, and graphene that is an extreme good conductor. The small band gap of the 1,3-ether configuration in saturated GO is yet another evidence that GO does not consists of 1,3-ether oxygens. A charge-transfer analysis (described in previous section) shows that the relative amount of charge flowing from carbon to oxygen atoms follows the structure's total energy, so that the lowest total energy also has the least charge exchange.

## V. SUMMARY AND CONCLUSIONS

It is evident from the foregoing analyses that 1,3-ether oxygens in GO are energetically not stable and therefore should not exist, irrespective of the amount of oxidation. There is the imaginary situation that a very high density of hydroxyls could obstruct the oxidation and leave oxygens no other choice than forming 1,3-ethers. However, the C/O ratio in experimentally synthesized GO is never less than 2, which means that there are always plenty of carbon atoms available during the oxidation to support the formation of 1,2-ether oxygens. It is therefore unlikely that, against all odds, 1,3-ether oxygens could appear in GO. The proposed structure of GO is one in which the 1,2-ether oxygen prevails and very close, but at the reverse side of the carbon plane, is the hydroxyl molecule. This arrangement repeats along the carbon network with subtle variations so that the oxidation over a macroscopic region appears as a random pattern.

By modeling GO in a DFT simulation, we have not only confirmed experimental findings, but in addition quantified these properties and found interesting new features. The carbon skeleton in GO with 1,2-ethers has a moderate wrinkling typically in the order of 0.5 Å. This deformation is mainly located around the hydroxyl molecules because of the locally induced $sp^3$ hybridization. The GO layers maintain a hexagonal structure that is close to graphene, despite the wrinkled geometry.

GO needs hydroxyl molecules to safeguard the stability of the structure, because the sole presence of 1,2-ether oxygens creates too much tension on the carbon grid. Intralayer hydrogen bonds between the hydroxyls and 1,2-ether oxygens are not relevant to a stable GO structure. However, hydrogen bonds via intercalated water molecules most probably are important in the interactions between the GO layers, which is a topic for further research.

The level of oxidation affects significantly the electronic structure of GO. At a low oxidation the band gap is small and gives GO the characteristics of a semiconductor. In addition, the existence of unpaired electrons should yield either ferro- or paramagnetic properties. At saturated oxidation levels the magnetic properties disappear and the band gap extends to figures closer to insulators.

## ACKNOWLEDGMENTS

This work was supported by the STAR faculty project in the Ministry of Education, and KOSEF through CNNC at SKKU. This research project was supported by WCU (World Class Univeristy) program through the Korea Science and Engineering Foundation funded by the Ministry of Education, Science and Technology (R31-2008-000-10029-0).

*Present address: University College, Sungkyunkwan University, Suwon 440-746, Korea; lahaye@skku.edu
†Present address: Institute of Basic Science, Sungkyunkwan University, Suwon 440-746, Korea
‡leeyoung@skku.edu; nanotube.skku.ac.kr

[1] K. Novoselov, A. Geim, S. Morozov, D. Jiang, Y. Zhang, S. Dubonos, I. Grigorieva, and A. Firsov, Science **306**, 666 (2004).
[2] K. Novoselov, A. Geim, A. Morozov, D. Jiang, M. Katsnelson, I. Grigorieva, S. Dubonos, and A. Firsov, Nature (London) **438**, 197 (2005).
[3] Y. Zhang, Y.-W. Tan, H. Stormer, and P. Kim, Nature (London) **438**, 201 (2005).
[4] C. Berger *et al.*, J. Phys. Chem. B **108**, 19912 (2004).
[5] S. Stankovich, D. Dikin, G. Dommett, K. Kohlhaas, E. Zimney, E. Stach, R. Piner, S. Nguyen, and R. Ruoff, Nature (London) **442**, 282 (2006).
[6] H. Schniepp, J.-L. Li, M. McAllister, H. Sai, M. Herrera-Alonso, D. Adamson, R. Prud'homme, R. Car, D. Saville, and I. Aksay, J. Phys. Chem. B **110**, 8535 (2006).
[7] S. Gilje, S. Han, M. Wang, K. Wang, and R. Kaner, Nano Lett. **7**, 3394 (2007).
[8] B. Brodie, Philos. Trans. R. Soc. London **149**, 249 (1859).
[9] U. Hofmann and R. Holst, Ber. Dtsch. Chem. Ges. B **72**, 754 (1939).
[10] G. Ruess, Monatsch. Chem. **76**, 381 (1947).
[11] A. Clauss, R. Plass, H. Boehm, and U. Hofmann, Z. Anorg. Allg. Chem. **291**, 205 (1957).
[12] W. Scholz and H. Boehm, Z. Anorg. Allg. Chem. **369**, 327 (1969).
[13] T. Nakajima, A. Mabuchi, and R. Hagiwara, Carbon **26**, 357 (1988).
[14] T. Nakajima and Y. Matsuo, Carbon **32**, 469 (1994).
[15] M. Mermoux, Y. Chabre, and A. Rousseau, Carbon **29**, 469 (1991).
[16] A. Lerf, H. He, M. Forster, and J. Klinowski, J. Phys. Chem. B **102**, 4477 (1998).
[17] T. Szabó, O. Berkesi, P. Forgó, K. Josepovits, Y. Sanakis, D. Petridis, and I. Dékány, Chem. Mater. **18**, 2740 (2006).
[18] A. Buchsteiner, A. Lerf, and J. Pieper, J. Phys. Chem. B **110**, 22328 (2006).
[19] D. Boukhvalov and M. Katsnelson, J. Am. Chem. Soc. **130**, 10697 (2008).
[20] A. Lerf, H. He, T. Riedl, M. Forster, and J. Klinowski, Solid State Ionics **101-103**, 857 (1997).
[21] H. He, T. Riedl, A. Lerf, and J. Klinowski, J. Phys. Chem. **100**, 19954 (1996).
[22] A. Lerf, A. Buchsteiner, J. Pieper, S. Schöttl, I. Dékány, T. Szabó, and H. Boehm, J. Phys. Chem. Solids **67**, 1106 (2006).
[23] W. Cai *et al.*, Science **321**, 1815 (2008).
[24] D. Sorescu, K. Jordan, and P. Avouris, J. Phys. Chem. B **105**, 11227 (2001).
[25] P. Giannozzi, R. Car, and G. Scoles, J. Chem. Phys. **118**, 1003 (2003).
[26] A. Incze, A. Pasturel, and P. Peyla, Phys. Rev. B **70**, 212103 (2004).
[27] J. L. Li, K. N. Kudin, M. J. McAllister, R. K. Prudhomme, I. A. Aksay, and R. Car, Phys. Rev. Lett. **96**, 176101 (2006).
[28] G. Kresse and J. Furthmüller, http://cms.mpi.univie.ac.at/vasp.
[29] P. E. Blochl, Phys. Rev. B **50**, 17953 (1994).
[30] G. Kresse and J. Furthmüller, Comput. Mater. Sci. **6**, 15 (1996).
[31] G. Kresse and J. Furthmuller, Phys. Rev. B **54**, 11169 (1996b).
[32] G. Kresse and D. Joubert, Phys. Rev. B **59**, 1758 (1999).
[33] J. P. Perdew, K. Burke, and M. Ernzerhof, Phys. Rev. Lett. **77**, 3865 (1996).
[34] J. P. Perdew, K. Burke, and M. Ernzerhof, Phys. Rev. Lett. **78**, 1396 (1997).
[35] J. P. Perdew, K. Burke, and M. Ernzerhof, Phys. Rev. Lett. **80**, 891 (1998).
[36] H. Monkhorst and J. Pack, Phys. Rev. B **13**, 5188 (1976).
[37] R. Feynman, Phys. Rev. **56**, 340 (1939).
[38] J. Musher, Am. J. Phys. **34**, 267 (1966).
[39] *C: The Art of Scientific Computing*, 2nd ed. (Cambridge University Press, Cambridge, 2002).
[40] H.-K. Jeong, Y. P. Lee, R. J. W. E. Lahaye, M.-H. Park, K. H. An, I. J. Kim, C.-W. Yang, C. Y. Park, R. S. Ruoff, and Y. H. Lee, J. Am. Chem. Soc. **130**, 1362 (2008).
[41] I. Jung, D. A. Dikin, R. D. Piner, and R. S. Ruoff, Nano Lett. **8**, 4283 (2008).